

ARTICLE

Received 12 Mar 2013 | Accepted 24 Jul 2013 | Published 16 Aug 2013

DOI: 10.1038/ncomms3346

Membrane-less hydrogen bromine flow battery

William A. Braff¹, Martin Z. Bazant² & Cullen R. Buie¹

In order for the widely discussed benefits of flow batteries for electrochemical energy storage to be applied at large scale, the cost of the electrochemical stack must come down substantially. One promising avenue for reducing stack cost is to increase the system power density while maintaining efficiency, enabling smaller stacks. Here we report on a membrane-less hydrogen bromine laminar flow battery as a potential high-power density solution. The membrane-less design enables power densities of 0.795 W cm^{-2} at room temperature and atmospheric pressure, with a round-trip voltage efficiency of 92% at 25% of peak power. Theoretical solutions are also presented to guide the design of future laminar flow batteries. The high-power density achieved by the hydrogen bromine laminar flow battery, along with the potential for rechargeable operation, will translate into smaller, inexpensive systems that could revolutionize the fields of large-scale energy storage and portable power systems.

¹Department of Mechanical Engineering, Massachusetts Institute of Technology, Cambridge, Massachusetts 02139, USA. ²Department of Chemical Engineering, Massachusetts Institute of Technology, Cambridge, Massachusetts 02139, USA. Correspondence and requests for materials should be addressed to C.R.B. (email: crb@mit.edu).

Low-cost energy storage remains a critical unmet need for a wide range of applications, including grid scale frequency regulation, load following, contingency reserves and peak shaving, as well as portable power systems^{1–4}. For applications that require the storage of large quantities of energy economically and efficiently, flow batteries have received renewed attention^{5,6}. A wide variety of solutions have been proposed, including zinc-bromine and vanadium redox cells^{1,7}. This includes recent efforts to incorporate novel concepts such as organic electrolytes for greater voltage stability and semisolid reactants for higher reactant energy density^{8,9} or chemistries to reduce reactant cost^{10,11}. One such permutation is the hydrogen bromine flow battery^{12–16}. The rapid and reversible reaction kinetics of both the bromine reduction reaction and the hydrogen oxidation reaction minimize activation losses^{17,18}, while the low cost ($\$1.39 \text{ kg}^{-1}$) and abundance (243,000 metric tons produced per year in the United States alone) of bromine distinguishes it from many other battery chemistries¹⁹. However, theoretical investigations of such systems have revealed that the perfluorosulfonic acid membranes typically used suffer from low conductivity in the absence of sufficient hydration^{20,21}. In the presence of hydrobromic acid, this membrane behaviour is the dominant limitation on overall performance^{22,15}.

Laminar flow electrochemical cells have been proposed to address many of the challenges that face traditional membrane-based systems^{23–29}. Laminar flow cells eliminate the need for an ion-exchange membrane by relying on diffusion to separate reactants. Eliminating the membrane decreases cost, relaxes hydration requirements and opens up the possibility for a much wider range of chemistries to be investigated. This flexibility has been exploited in the literature; examples include vanadium redox flow batteries^{23,27}, methanol²⁵, formic acid²⁴ and hydrogen fuel cells²⁹. However, none of these systems have achieved power densities as high as their membrane-based counterparts. This is largely because the proposed chemistries already work well with existing membrane technologies that have been refined and optimized over several decades. More recently, a laminar flow fuel cell based on borohydride and cerium ammonium nitrate employed a porous separator, chaotic mixing and consumption of acid and base to achieve a power density of 0.25 W cm^{-2} (ref. 30). This appears to be the highest previously published power density for a membrane-less laminar flow fuel cell.

In this work, we present a membrane-less hydrogen bromine laminar flow battery (HBLFB) with reversible reactions and a peak power density of 0.795 W cm^{-2} at room temperature and atmospheric pressure. The cell uses a membrane-less design similar to previous work²⁵, but with several critical differences that allow it to triple the highest previously reported power density for a membrane-less electrochemical cell and also enable recharging. First, where many previous laminar flow electrochemical cell designs were limited to low current operation by the low oxygen concentration at the cathode, the HBLFB uses gaseous hydrogen fuel and aqueous bromine oxidant^{23–26,29}. This allows for high concentrations of both reactants at their respective electrodes, greatly expanding the mass-transfer capacity of the system. Next, both reactions have fast, reversible kinetics, with no phase change at the liquid electrode, eliminating bubble formation as a design limitation. These two characteristics of the HBLFB enable high-power density storage and discharge of energy at high efficiency, while avoiding the cost and reliability issues associated with membrane-based systems.

Results

Numerical model. A two-dimensional numerical model of the device was constructed to allow for a greater understanding of the

underlying physics of the cell^{31,32}. The model solves the Nernst–Planck equations with advection in the imposed flow for the concentrations and electrostatic potential, assuming a quasi-neutral bulk electrolyte. Fully developed Poiseuille flow was assumed in the channel, with reactions occurring at the top and bottom of the channel along thin electrodes (Fig. 1). Because the channel width far exceeds the height, edge effects can be ignored, validating the two-dimensional assumption. Equilibrium potentials along the cathode and anode were determined by the Nernst equation assuming dilute solution theory, and activation losses were estimated using the symmetric Butler–Volmer equation, consistent with existing kinetics data¹⁷. Electrolytic conductivity was assumed to depend on the local (spatially evolving) hydrobromic acid concentration and was calculated using empirical data³³.

Discharge experiments. The cell was operated galvanostatically at room temperature and atmospheric pressure over a range of flow rates and reactant concentrations. The cell was observed to reach steady state in $<10 \text{ s}$, thus each data point was collected after 60 s of steady-state operation to eliminate transient artifacts. Polarization data were collected as a function of Peclet number (Pe) for the HBLFB using 1 M HBr and 1 M Br_2 and compared with numerical model results (Fig. 2). The Peclet numbers of

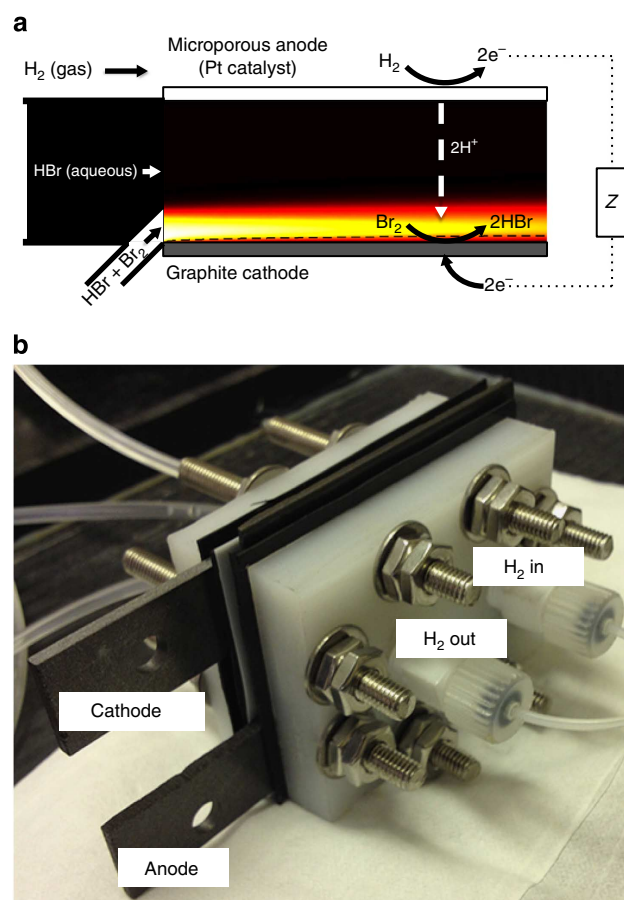


Figure 1 | Schematic of reactant flow within the HBLFB. During discharge, liquid bromine is reduced to hydrobromic acid along the lower solid graphite electrode, and hydrogen is oxidized at the upper porous electrode. (a) Numerically predicted concentration of Br_2 for a Pe of 10,000 and initial concentrations of bromine and hydrobromic acid of 1 M are overlaid. (b) Assembled cell before testing.

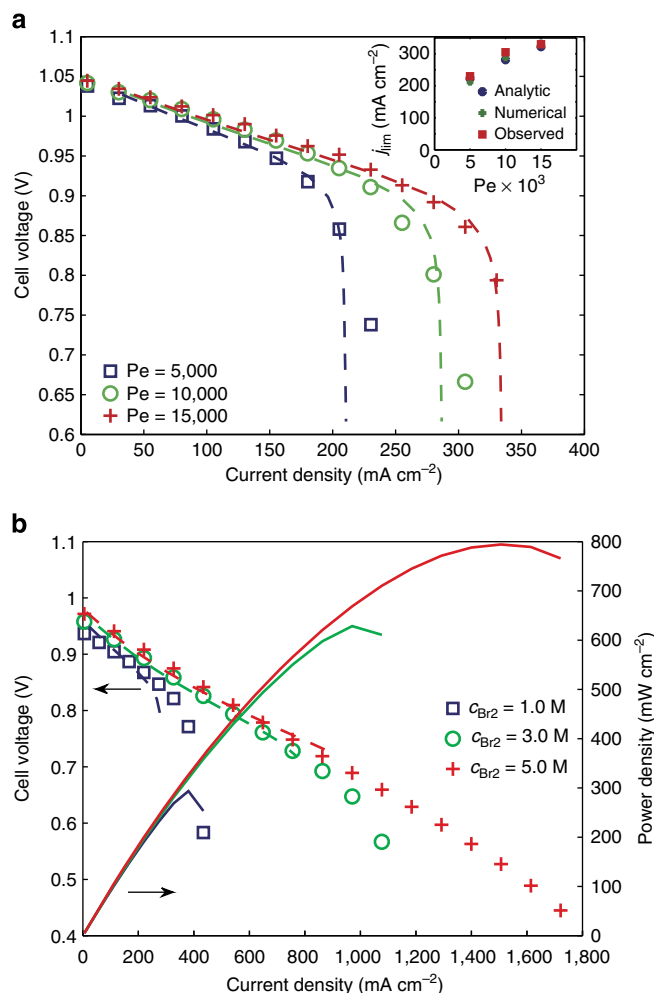


Figure 2 | Discharge performance of the HBLFB. Predicted (dashed) and observed (symbols) cell voltage as a function of current density and Pe for the HBLFB during discharge using 1M Br₂ and 1M HBr. For low-concentration reactants, mass transport is the dominant source of loss, and limiting current density j_{lim} can be predicted analytically as a function of Pe using the L  v  que approximation (inset). **(a)** Predicted (dashed) and observed (symbols) cell voltage and power density as a function of current density and Br₂ concentration for Pe = 10,000 and 3M HBr. The higher reactant concentrations require concentrated solution theory to accurately model, but allow for much higher current and power density **(b)**.

5,000, 10,000 and 15,000 correspond to Reynolds numbers of 5.75, 11.5 and 17.25, oxidant flow rates of 0.22, 0.44 and 0.66 ml min⁻¹ cm⁻² and mean velocities of 6.3, 12 and 19 mm s⁻¹, respectively. The oxidant flow rates correspond to stoichiometric currents of 0.7, 1.4 and 2.1 A cm⁻² respectively. Hydrogen was flowed in excess at a rate of 25 sccm. The slightly enhanced maximum current density of the observed results compared with the predicted results may be attributed to the roughness of the electrode surface producing chaotic mixing that slightly enhances reactant transport. Below limiting current, the agreement between model and experiment is very good. At low current densities, the voltage differences between the different Peclet numbers are small; however, in each case, the voltage drops rapidly as the cell approaches limiting current, corresponding to the predicted mass-transfer limitations.

Analytical limiting current. These limitations can be estimated analytically for fast reactions by assuming a bromine

concentration of zero at the cathode and applying the L  v  que approximation to the bromine depletion layer^{34,35}. For a channel of length L and height h , fully developed Poiseuille flow and initial bromine concentration c_0 , the resulting partial differential equation and boundary conditions can be expressed in terms of dimensionless bromine concentration $\tilde{c} = c/c_0$, position $\tilde{y} = y/h$ and $\tilde{x} = x/h$, channel aspect ratio $\beta = L/h$ and $Pe = Uh/D$.

$$\frac{6Pe}{\beta} \tilde{y} \frac{\partial \tilde{c}}{\partial \tilde{x}} = \frac{\partial^2 \tilde{c}}{\partial \tilde{y}^2} \quad (1)$$

$$\tilde{c}(\tilde{x} = 0) = 1 \quad (2)$$

$$\tilde{c}(\tilde{y} \rightarrow \infty) = 1 \quad (3)$$

$$\tilde{c}(\tilde{y} = 0) = 0 \quad (4)$$

A similarity technique can be applied to convert this to an ordinary differential equation.

$$\eta^2 \frac{\partial \tilde{c}}{\partial \eta} = \frac{\partial^2 \tilde{c}}{\partial \eta^2} \quad (5)$$

$$\tilde{c}(\eta = 0) = 0 \quad (6)$$

$$\tilde{c}(\eta \rightarrow \infty) = 1 \quad (7)$$

$$\eta = \frac{\tilde{y}}{\sqrt[3]{\beta \tilde{x}/2Pe}} \quad (8)$$

This equation can be solved exactly in terms of the incomplete Gamma function, $\Gamma(s, a)$.

$$\tilde{c}(\tilde{x}, \tilde{y}) = \Gamma\left(\frac{2Pe\tilde{y}^3}{3\beta\tilde{x}}, \frac{1}{3}\right) \quad (9)$$

Limiting current can be calculated using Faraday's law to determine the distribution of current along the length of the electrode and integrating to obtain limiting current j_{lim} as a function of Pe, reactant concentration c_0 and diffusivity D , channel height h and aspect ratio β , Faraday's constant F , and the number of moles of electrons transferred per mole of reactant n .

$$j_{lim} = 1.47 \frac{c_0 n D F}{h} \sqrt[3]{\frac{Pe}{\beta}} \quad (10)$$

This result has considerable bearing on how laminar flow systems should be designed and operated. The presence of aspect ratio in the denominator means that shortening the channel results in greater power density, as observed in experiment³⁶. In addition, the weak 1/3 dependence on Pe means that increasing the flow rate beyond a certain point yields minimal benefits. There was excellent agreement between maximum observed current density, maximum numerically predicted current density and the analytically predicted limiting current density as a function of Pe (Fig. 2a).

High-power operation. Higher bromine concentrations were also investigated by using a more concentrated electrolyte (3M HBr) to enhance bromine solubility and move beyond the mass-transfer limitations of 1 M Br₂. The performance of this system was investigated at a Pe of 10,000 by varying the bromine concentration (Fig. 2b). Using 5 M Br₂ and 3 M HBr as the oxidant and electrolyte, respectively, a peak power density of 0.795 W cm⁻² was observed when operated near limiting current density. This corresponds to power density per catalyst loading of 1.59 W mg⁻¹ platinum. The open-circuit potential of the cell dropped more than might be predicted simply using the Nernst equation at the cathode. The drop in open-circuit potential is consistent with data on the activity coefficient of concentrated

hydrobromic acid available in the literature, as well as previous studies that employed concentrated hydrobromic acid^{14,33}. To account for this effect, empirical data for the activity coefficient of hydrobromic acid as a function of local concentration was incorporated into the boundary conditions. The activity coefficient was assumed to vary slowly enough within the electrolyte that gradients in activity coefficient were neglected in the governing equations. Taking into account the activity coefficient of hydrobromic acid, there is good agreement between the model and experiment. As in the low-concentration data, the observed maximum current density is slightly higher than predicted. Otherwise, the model captures the main features of the data, including the transition from transport-limited behaviour at low bromine concentrations, evidenced by a sharp drop in cell voltage, to ohmically limited behaviour at high bromine concentrations. In this ohmically limited regime, mass-transport limitations are less important, and the limiting current solution applied to the low-concentration results does not apply.

Recharging and round-trip efficiency. Charging behaviour was also investigated by flowing only HBr and applying a voltage to electrolyse HBr back into Br₂ and H₂. The voltage versus current density behaviour of the cell was investigated during charging as a function of HBr concentration at a Pe of 10,000 (Fig. 3). Experimental conditions were kept identical to those of the discharge experiments, with the exception that no bromine was externally delivered to the cell. Side reactions, in particular the formation of hypobromous acid and the evolution of oxygen, become dominant before potentials get sufficiently high to observe limiting current; the numerical model cannot accurately describe this behaviour at potentials >1.3 volts and was not applied to the charging data. At lower voltages, both the electrolyte conductivity and the limiting current density were increased by increasing the HBr concentration, resulting in increased performance (Fig. 3). Round-trip voltage efficiency was then calculated by dividing the discharge voltage by the charging voltage for a number of reactant concentrations (Fig. 4). Voltage efficiencies slightly >100% were observed for low-power densities due to differences in the open-circuit potential that are generated by the variation in bromine concentration between the charging and discharging experiments, but this anomaly becomes unimportant at higher current densities, where the reactant concentration varies spatially much more strongly. Using high-concentration reactants, round-trip efficiency of 90% was observed when using high-concentration reactants at 25% of peak power (200 mW cm⁻² during discharge). This appears to be the first publication of round-trip charging and discharging of a membrane-less laminar flow battery, and compares very favourably to existing flow battery technologies. Vanadium redox batteries, for example, have demonstrated voltage efficiencies as high as 91%, but only at a discharge power density nearly an order of magnitude lower than the HBLFB³⁷.

Although closed-loop operation was not demonstrated in this study, some insight into coulombic efficiency can be gathered by considering the effect of reactant mixing within the channel. At 25% of peak power, the single-pass coulombic efficiency of the cell is only about 1%. If no attempt was made to separate the reactants at the outlet of the cell, the resulting energy efficiency of the cell would also be very low. However, if the channel outlet was split to conserve the volume of stored electrolyte and oxidant, only the Br₂ that had diffused into the electrolyte layer would be lost. Assuming fully developed Poiseuille flow, this corresponds to a coulombic efficiency of 72% or a round-trip energy efficiency of 66%.

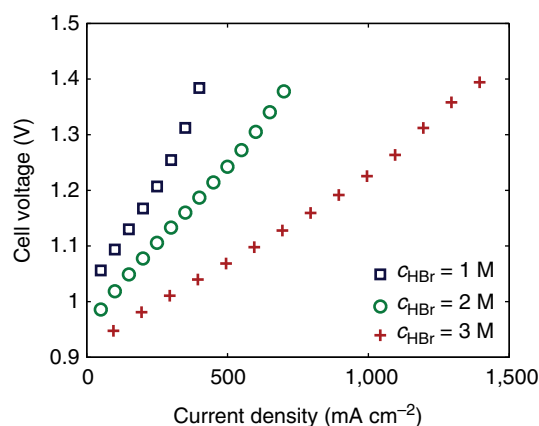


Figure 3 | Charging performance of the HBLFB. Observed cell voltage during charging as a function of HBr concentration at a Pe of 10,000 and a Br₂ concentration of 1 M. Increasing the HBr concentration increases both the conductivity and the limiting current, resulting in superior performance.

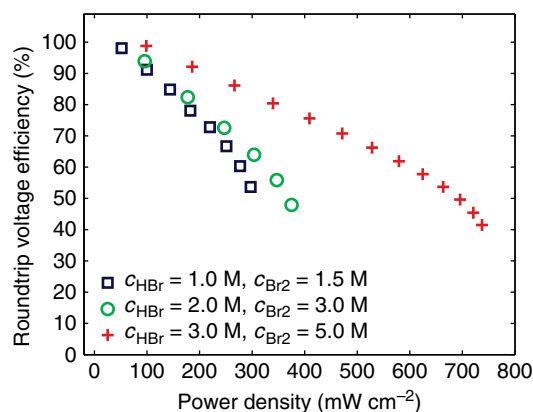


Figure 4 | Round-trip efficiency of the HBLFB. Round-trip voltage efficiency of the HBLFB as a function of power density for a range of reactant concentrations at a Pe of 10,000.

Discussion

Several opportunities for improvement on this design remain to be investigated. First, the porous hydrogen anode was selected because of its commercial availability, despite the fact that it was intended for use in a proton-exchange membrane fuel cell. The catalyst composition and structure, wettability, and media porosity have not been optimized. Previous work has shown that these parameters can have an impact on the power density of laminar flow cells by nearly an order of magnitude³⁸. Recent work on thin hydrogen oxidation electrodes has demonstrated that excellent catalytic activity can be achieved with platinum loadings as low as 3 μg cm⁻², more than two orders of magnitude lower than the electrodes used in this study³⁹. Assuming equivalent performance, an HBLFB employing such a hydrogen electrode would have a specific power density of roughly 250 W mg⁻¹ platinum, virtually eliminating platinum as a cost-limiting component of the system. Second, the channel geometry used in these experiments was relatively long to achieve high-oxidant utilization. Shortening the channel would decrease the average thickness of the depletion layer that develops along the cathode, enabling higher current densities³⁶. Third, reducing the distance between electrodes would greatly reduce ohmic losses, which are dominant when high-concentration reactants are fed into the cell. Incorporating further refinements, such as micropatterned chaotic mixing patterns,

coupled with a non-specific convection barrier or non-noble metal catalysts could also improve performance^{30,40,41}.

The initial data presented here for the HBLFB suggest that high-power density and high-efficiency energy storage are achievable using a membrane-less electrochemical cell operating at room temperature and pressure. The HBLFB requires no special procedures or facilities to fabricate and uses kinetically favourable reactions between abundant, low-cost reactants. Recent work has shown that a membrane-based hydrogen-bromine flow battery at room temperature can generate 850 mW cm^{-2} , or 7% more power than these experiments with the HBLFB at room temperature¹⁶. However, this was achieved using a stoichiometric oxidant flow rate over eight times larger than that used in this work, as well as an acid-treated porous bromine electrode with substantially greater active area than the bare graphite bromine electrode of the HBLFB.

This work represents a major advance of the state-of-the-art in flow batteries. To the best of the authors' knowledge, the data presented here represent the highest power density ever observed in a laminar flow electrochemical cell by a factor of three, as well as some of the first recharging data for a membrane-less laminar flow electrochemical cell^{30,42}. Although previous work has identified the appropriate scaling laws^{43,44}, the result presented here represents the first exact analytical solution for limiting current density applied to a laminar flow electrochemical cell, and serves as a guide for future designs. The HBLFB rivals the performance of the best membrane-based systems available today without the need for costly ion-exchange membranes, high-pressure reactants or high-temperature operation. This system has the potential to have a key role in addressing the rapidly growing need for low-cost, large-scale energy storage and high-efficiency portable power systems.

Methods

Cell fabrication. A proof-of-concept electrochemical cell was assembled using a graphite cathode and a commercial carbon cloth gas diffusion anode with 0.5 mg cm^{-2} of platinum (60% supported on carbon) obtained from the Fuel Cell Store (San Diego, CA). The cell was housed between graphite current collectors and polyvinylidene fluoride porting plates (Fig. 1b). All components were fabricated using traditional CNC machining or die cutting. No additional catalyst was applied to the cathode. The hydrogen flow rate through the porous anode was 25 sccm , and an oxidant stream of bromine mixed with aqueous hydrobromic acid passed through the channel in parallel with an electrolyte stream of aqueous hydrobromic acid. An $800\text{-}\mu\text{m}$ thick Viton gasket was used to separate the two electrodes and create the channel, which was 1.4 cm long from oxidant inlet to outlet with an active area of 25 mm^2 . A fixed ratio of 10:1 was maintained between the electrolyte and oxidant flow rates, and the net flow rate was adjusted to study the performance of the cell as a function of the Pe defined by the average flow velocity U , channel height h and bromine diffusion coefficient D such that $\text{Pe} \equiv Uh/D$.

Numerical model details. A scaled, dimensionless model was constructed in COMSOL Multiphysics, and results were calculated over a range of flow rates and reactant concentrations. A complete description of the model has been presented previously^{31,32}. Bromine concentration varied along the length of the channel, resulting in strong spatial variations in the current density (Fig. 1a). Current-voltage data were obtained for a range of reactant concentrations and flow rates for comparison with experimental data by averaging the current density along the length of the cell and by calculating solutions over a range of specified cell voltages.

References

- Yang, Z. *et al.* Electrochemical energy storage for green grid. *Chem. Rev.* **111**, 3577–3613 (2011).
- Rugolo, J. & Aziz, M. J. Electricity storage for intermittent renewable sources. *Energy Environ. Sci.* **5**, 7151–7160 (2012).
- Soloveichik, G. L. Battery technologies for large-scale stationary energy storage. *Annu. Rev. Chem. Biomol. Eng.* **2**, 503–527 (2011).
- Hittinger, E., Whitacre, J. F. & Apt, J. What properties of grid energy storage are most valuable? *J. Power Sources* **206**, 436–449 (2012).
- Weber, A. Z. *et al.* Redox flow batteries: a review. *J. Appl. Electrochem.* **41**, 1137–1164 (2011).
- Ponce de León, C., Fras-Ferrer, A., González-García, J., Szánto, D. A. & Walsh, F. C. Redox flow cells for energy conversion. *J. Power Sources* **160**, 716–732 (2006).
- Knehr, K. W., Agar, E., Dennison, C. R., Kalidindi, A. R. & Kumbur, E. C. A transient vanadium flow battery model incorporating vanadium crossover and water transport through the membrane. *J. Electrochem. Soc.* **159**, A1446–A1459 (2012).
- Liu, Q. *et al.* Non-aqueous chromium acetylacetonate electrolyte for redox flow batteries. *Electrochem. Commun.* **12**, 1634–1637 (2010).
- Duduta, M. *et al.* Semi-solid lithium rechargeable flow battery. *Adv. Energy Mater.* **1**, 511–516 (2011).
- Skyllas-Kazacos, M., Kasherman, D., Hong, D. R. & Kazacos, M. Characteristics and performance of 1-Kw unsw vanadium redox battery. *J. Power Sources* **35**, 399–404 (1991).
- Wang, W. *et al.* A new Fe/V redox flow battery using a sulfuric/chloric mixed-acid supporting electrolyte. *Adv. Energy Mater.* **2**, 487–493 (2012).
- Kosek, J. A. & LaConti, A. B. Advanced hydrogen electrode for a hydrogen bromine battery. *J. Power Sources* **22**, 293–300 (1988).
- Yeo, R. S. & Chin, D.-T. Hydrogen-bromine cell for energy-storage applications. *J. Electrochem. Soc.* **127**, 549–555 (1980).
- Livshits, V., Ulus, A. & Peled, E. High-power H_2/Br_2 fuel cell. *Electrochem. Commun.* **8**, 1358–1362 (2006).
- Kreutzer, H., Yarlagadda, V. & Nguyen, T. V. Performance evaluation of a regenerative hydrogen-bromine fuel cell. *J. Electrochem. Soc.* **159**, F331–F337 (2012).
- Cho, K. T. *et al.* High performance hydrogen/bromine redox flow battery for grid-scale energy storage. *J. Electrochem. Soc.* **159**, A1806–A1815 (2012).
- Cooper, W. & Parsons, R. Kinetics of bromine/bromide electrode on platinum in aqueous sulphuric acid. *Trans. Faraday Soc.* **66**, 1698–1712 (1970).
- Goor-Dar, M., Travitsky, N. & Peled, E. Study of hydrogen redox reactions on platinum nanoparticles in concentrated HBr solutions. *J. Power Sources* **197**, 111–115 (2012).
- U S Geological Survey. Mineral Commodity Summaries 2011. Tech. Rep. 198, US Geological Survey (2011).
- Clark, J. K., Paddison, S. J., Eikerling, M., Dupuis, M. & Zawodzinski, T. A. A comparative ab initio study of the primary hydration and proton dissociation of various imide and sulfonic acid ionomers. *J. Phys. Chem. A* **116**, 1801–1813 (2012).
- Kreuer, K.-D., Paddison, S. J., Spohr, E. & Schuster, M. Transport in proton conductors for fuel-cell applications: simulations, elementary reactions, and phenomenology. *Chem. Rev.* **104**, 4637–4678 (2004).
- Savinell, R. F. & Fritts, S. D. Theoretical performance of a hydrogen bromine rechargeable spe fuel-cell. *J. Power Sources* **22**, 423–440 (1988).
- Ferrigno, R., Stroock, A. D., Clark, T. D., Mayer, M. & Whitesides, G. M. Membraneless vanadium redox fuel cell using laminar flow. *J. Am. Chem. Soc.* **124**, 12930–12931 (2002).
- Chohan, E. R., Markoski, L. J., Wieckowski, A. & Kenis, P. J. A. Microfluidic fuel cell based on laminar flow. *J. Power Sources* **128**, 54–60 (2004).
- Jayashree, R. S. *et al.* Air-breathing laminar flow-based microfluidic fuel cell. *J. Am. Chem. Soc.* **127**, 16758–16759 (2005).
- Cohen, J. L., Westly, D. A., Pechenik, A. & Abruña, H. D. Fabrication and preliminary testing of a planar membraneless microchannel fuel cell. *J. Power Sources* **139**, 96–105 (2005).
- Kjeang, E. *et al.* High-performance microfluidic vanadium redox fuel cell. *Electrochim. Acta* **52**, 4942–4946 (2007).
- Kjeang, E., Michel, R., Harrington, D. A., Djilali, N. & Sinton, D. A microfluidic fuel cell with flow-through porous electrodes. *J. Am. Chem. Soc.* **130**, 4000–4006 (2008).
- Brushett, F. R., Zhou, W. -P., Jayashree, R. S. & Kenis, P. J. A. Alkaline microfluidic hydrogen-oxygen fuel cell as a cathode characterization platform. *J. Electrochem. Soc.* **156**, B565 (2009).
- Da Mota, N. *et al.* Membraneless, room-temperature, direct borohydride/cerium fuel cell with power density of over 0.25 W/cm^2 . *J. Am. Chem. Soc.* **134**, 6076–6079 (2012).
- Braff, W. A. & Buie, C. R. Hydrogen bromine laminar flow electrochemical cell for high power and efficiency energy storage applications. *ECS Trans.* **33**, 179–190 (2011).
- Braff, W. A., Buie, C. R. & Bazant, M. Z. Numerical and analytic modeling of a membraneless hydrogen bromine laminar flow battery. *ECS Trans.* **53**, 51–62 (2013).
- Lide, D. R. *Handbook of Chemistry and Physics* (CRC Press, 2012).
- Lévêque, A. *Les Lois de la Transmission de Chaleur par Convection* (Annales des Mines ou Recueil de Mémoires sur l'Exploitation des Mines et sur les Sciences et les Arts qui s'y Rattachent, 1928).
- Probstein, R. F. *Physicochemical Hydrodynamics* (Wiley-Interscience, 1989).
- Thorson, M. R., Brushett, F. R., Timberg, C. J. & Kenis, P. J. A. Design rules for electrode arrangement in an air-breathing alkaline direct methanol laminar flow fuel cell. *J. Power Sources* **218**, 28–33 (2012).

37. Haddadi-Asl, V., Kazacos, M. & Skyllas-Kazacos, M. Conductive carbon-polypropylene composite electrodes for vanadium redox battery. *J. Appl. Electrochem.* **25**, 29–33 (1995).
38. Brushett, F. R., Naughton, M. S., Ng, J. W. D., Yin, L. & Kenis, P. J. A. Analysis of Pt/C electrode performance in a flowing-electrolyte alkaline fuel cell. *Int. J. Hydrogen Energ.* **37**, 2559–2570 (2012).
39. Wesselmack, M., Wickman, B., Lagergren, C. & Lindbergh, G. Hydrogen oxidation reaction on thin platinum electrodes in the polymer electrolyte fuel cell. *Electrochem. Commun.* **12**, 1585–1588 (2010).
40. Stroock, A. D. *et al.* Chaotic mixer for microchannels. *Science* **295**, 647–651 (2002).
41. Liu, R.-F. *et al.* Theory Guided Design of Electrocatalysts for the H₂-Br₂ Flow Battery System. 221st ECS Meeting, Seattle, WA, 2012.
42. Lee, J. W., Goulet, M.-A. & Kjeang, E. Microfluidic redox battery. *Lab. Chip.* **13**, 2504–2507 (2013).
43. Ismagilov, R. F., Stroock, A. D., Kenis, P. J. A., Whitesides, G. & Stone, H. A. Experimental and theoretical scaling laws for transverse diffusive broadening in two-phase laminar flows in microchannels. *Appl. Phys. Lett.* **76**, 2376 (2000).
44. Bazylak, A., Sinton, D. & Djilali, N. Improved fuel utilization in microfluidic fuel cells: a computational study. *J. Power Sources* **143**, 57–66 (2005).

Acknowledgements

We acknowledge financial support from the Department of Defense (DoD) through the National Defense Science and Engineering Graduate Fellowship (NDSEG) Program, as well as the MIT Energy Initiative Seed Fund.

Author contributions

W.A.B. performed the experiments and simulations. M.Z.B. developed the theoretical plan, and C.R.B. developed the experimental plan. All authors wrote and edited the manuscript.

Additional information

Competing financial interests: The authors declare no competing financial interests.

Reprints and permission information is available online at <http://npg.nature.com/reprintsandpermissions/>

How to cite this article: Braff, W. A. *et al.* Membrane-less hydrogen bromine flow battery. *Nat. Commun.* **4**:2346 doi: 10.1038/ncomms3346 (2013).